

# Analytical Solution for Estimation of Temperature-Dependent Material Properties of Metals Using Modified Morse Potential

Kuo-Ning Chiang<sup>1</sup>, Chan-Yen Chou<sup>2</sup>, Chung-Jung Wu<sup>2</sup>  
Chao-Jen Huang<sup>2</sup> and Ming-Chih Yew<sup>2</sup>

**Abstract:** An atomic-level analytical solution, together with a modified Morse potential, has been developed to estimate temperature-dependent thermal expansion coefficients (CTE) and elastic characteristics of bulk metals. In this study, inter-atomic forces are considered as a set of anharmonic oscillator networks which can be described by Morse potential, while the material properties can be defined by these inter-atomic forces; when temperature increases, the vibration of the anharmonic oscillator causes the phenomenon of temperature-dependent material properties. The results of analysis showed that the original Morse potential can give a reasonable prediction of the thermal expansion coefficients and elastic constants of metals at room temperature; however, it has difficulties in giving an accurate result at low and high temperatures. Therefore, to overcome the deficiency, a temperature-dependent modified Morse potential is developed and validated with various metals.

**Keyword:** CTE, Elastic constant, Morse potential

## 1 Introduction

Potential functions are developed to simplify the complexity of quantum mechanics-based computation such as *ab initio* calculations. These functions return a value of energy based on the conformation of the molecules or atoms. Some potentials such as Morse potential [Girifalco and Weizer (1959)] and embedded-atom method (EAM) [Daw and Baskes (1984)] have been proposed to describe the potential energy of metal atoms. They have been applied successfully in a number of studies

---

<sup>1</sup> Corresponding author. Advanced Microsystem Packaging and Nano-Mechanics Research Laboratory, Power Mechanical Engineering Dept., National Tsing-Hua University, 101 Sec. 2, Kuang-Fu Rd., Hsinchu, Taiwan 300, R. O. C.

<sup>2</sup> Research assistant. Advanced Microsystem Packaging and Nano-Mechanics Research Laboratory, Power Mechanical Engineering Dept., National Tsing-Hua University, Taiwan

to estimate the material properties of metals at room temperature in many articles [Chiang, Chou, Wu and Yuan (2006); Foiles and Daw (1988); Jeng and Tan (2002); Park, Cho, Kim, Jun and Im (2006); Theodosiou and Saravanos (2007)]. However, there are some difficulties in predicting the thermal and mechanical behaviors of metals when the temperature condition deviates from room temperature.

Chemical bonds are also treated as anharmonic oscillators. The summation of the potential and kinetic energy of the oscillator remains a constant and is as a function of temperature. The vibrate-kinetic energy reaches the maximum status as the stretched/compressed potential energy is in the minimum state, the same way that the potential energy reaches the maximum status as the kinetic energy is in the minimum state. Temperature is the physical quantity that implies atomic vibration, resulting in the shift of the anharmonic vibration center when the temperature increases. Likewise, it causes the phenomenon of thermal expansion, which is a temperature-dependent behavior. Moreover, other material characteristics of solids, such as elastic constant and heat capacity, also vary with temperature due to the nature of anharmonic vibrations. Furthermore, molecular or atomic bonding strengths are presented after taking the differentiation of the potential function. Bonding strengths are the key factors of the mechanical properties of bulk materials.

Based on the simple-spring-single-lattice (SSSL) calculation [Chiang, Chou, Wu and Yuan (2006)], this study presents the development of an atomic-level analytical solution together with a modified Morse potential are developed in estimating temperature-dependent thermal expansion coefficients (CTE) and elastic characteristics of bulk metals. A set of metal elements with its Morse potential parameters is investigated. This model provides an efficient and rapid way for evaluating material characteristics once the parameters of potential function and temperature are determined. At the same time, a temperature-dependent modified Morse potential is also developed and validated with various metals.

## 2 Temperature-Dependent Thermal Expansion Coefficient Calculation

Considering the diatom system shown in Fig. 1, two atoms are bonded together by an atomic pseudo spring with proper potential energy. The atoms are stationary at absolute zero, and they start to vibrate as temperature increases. At temperature  $T$ , the disturbing (increased) energy  $\Delta E$  of one-dimensional diatom motion is described as  $1/2k_B T$ , where  $k_B$  represents Boltzmann's constant.  $\Delta E$  represents the disturbing energy of diatom vibration with the repulse and attractive vibration amplitudes  $r_1$  and  $r_2$ , the average distance of this diatom system changes from  $r_0$  to  $(r_2 - r_1)/2$  when the temperature increases from  $T_1$  K to  $T_2$  K. In comparison with experimental data,  $T_1$  is set to be 0 K in this study. Therefore, the thermal expansion

coefficient of the diatom system is described as following:

$$CTE = \frac{\frac{(r_2 - r_1)}{2} - r_0}{r_0(T_2 - T_1)} \quad (1)$$

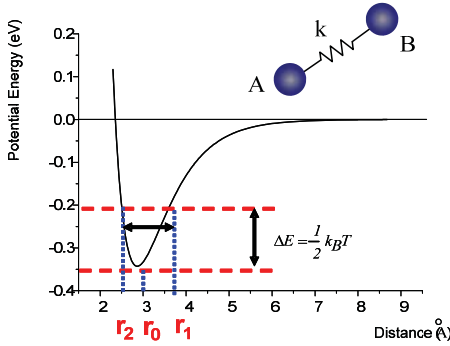


Figure 1: A sketch of CTE calculation model

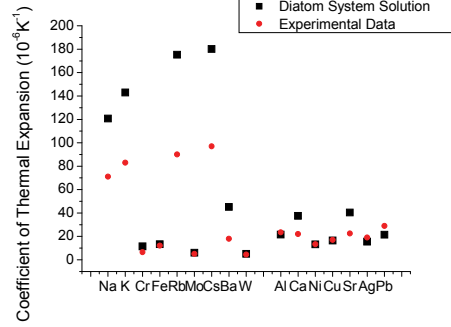


Figure 2: The calculated coefficient of thermal expansion of metals with experimental validation

In this study, Morse potential function, which illustrates the bond strength of the diatom system and which has been used for more than 70 years, is adopted. It can describe the relationship of potential energy versus diatom distance, as well as depict the relationship of bond strength versus diatom distance. The potential energy  $E(r_{ij})$  of two atoms  $i$  and  $j$  separated by a distance  $r_{ij}$  is expressed as following:

$$E(r_{ij}) = D \left[ e^{-2\alpha(r_{ij}-r_0)} - 2e^{-\alpha(r_{ij}-r_0)} \right] \quad (2)$$

where  $D$  is the dissociation energy of the diatom system,  $r_0$  is the equilibrium length, and  $\alpha$  is a constant with the dimension of reciprocal distance. By applying Eq. (2), one can determine the disturbing energy  $\Delta E$  when temperature increases from 0 K to  $T$  K as shown in Eq. (3):

$$D \left( e^{-2\alpha(r_{ij}-r_0)} - 2e^{-\alpha(r_{ij}-r_0)} \right) + D = \frac{1}{2} k_B T \quad (3)$$

By solving Eq. (3), the vibration amplitudes  $r_1$  and  $r_2$  are determined; therefore, the CTE defined by Eq. (1) becomes

$$r_1 = \frac{\alpha r_0 - \ln \left( 1 - \sqrt{\frac{k_B T}{2D}} \right)}{\alpha}, \quad r_2 = \frac{\alpha r_0 - \ln \left( 1 + \sqrt{\frac{k_B T}{2D}} \right)}{\alpha} \quad (4)$$

$$CTE = \frac{- \left[ \ln \left( 1 + \sqrt{\frac{k_B T}{2D}} \right) + \ln \left( 1 - \sqrt{\frac{k_B T}{2D}} \right) \right]}{2\alpha r_0 T} \quad (5)$$

Equation (5) shows that the coefficient of thermal expansion of metals can be estimated simply by three Morse potential parameters, namely,  $\alpha$ ,  $D$ ,  $r_0$ , and the disturbing energy which is represented in the form of temperature  $T$ . Girifalco and Weizer [Girifalco and Weizer (1959)] calculated the Morse potential parameters for cubic metals using the experimental values of the energy of vaporization, the lattice constant, and the compressibility. Table I shows the Morse parameters for cubic metals applied in this study and presents two groups of the metallic lattice structure that can be categorized. One is the body-centered cubic (BCC) structure including Na, K, Cr, Fe, Rb, Mo, Cs, Ba, and W, while the other is the face-centered cubic (FCC) structure including Al, Ca, Ni, Cu, Sr, Ag and Pb.

In Girifalco's potential model, the dissociation energy is explicitly associated with two energy equations in equilibrium, and one experimental compressibility relation. Therefore, the Morse potential is treated as a semi-empirical formulation. After substituting Morse potential parameters of Table I into Eq. (5), the CTE of metals at room temperature is obtained as shown in Fig. (2). The calculated CTE shows reasonable agreement with the experimental one [Davis (1990); Gray (1973); Lide (2002)].

Applying further Eq. (5) to calculate the CTE at different temperatures, the results become insensitive to temperature and the prediction does not match experimental results anymore. Figure (3) shows the comparison of the temperature-dependent thermal expansion coefficients of Fe, Al, Ag, Ca, and Ni metals. In reality, the CTE of metals is much smaller at a low temperature than that at room temperature, and CTE becomes larger when the temperature is close to the melting point. This is due to the changes in bond strength and shifting of the average position of atomic vibration. However, in the analytical solution using original Morse potential, the calculated CTE is insensitive with temperature which does not fit the natural thermal behavior of metals. Therefore, a modified Morse potential function with temperature-dependent parameters is a must in describing the thermal expansion behavior of metals.

There are two terms in the original Morse potential function, one representing the attractive energy and the other representing the repulsive energy between atoms. In order to fully describe the thermomechanical characteristics, it is deduced that a temperature-related parameter should be included in the Morse potential. A modi-

Table 1: The Morse potential parameters constructed by Girifalco and Weizer<sup>1</sup>

Metal	$r_0 = \text{\AA}$	$D$ (eV)	$\alpha = \text{\AA}^{-1}$
Na	5.336	0.06334	0.58993
K	6.369	0.05424	0.49767
Cr	2.754	0.4414	1.5721
Fe	2.845	0.4174	1.3885
Rb	7.207	0.04644	0.42981
Mo	2.976	0.8032	1.5079
Cs	7.557	0.04485	0.41569
Ba	5.373	0.1416	0.65698
W	3.032	0.9906	1.4116
Al	3.253	0.2703	1.1646
Ca	4.569	0.1623	0.80535
Ni	2.78	0.4205	1.4199
Cu	2.866	0.3429	1.3588
Sr	4.988	0.1513	0.73776
Ag	3.115	0.3323	1.369

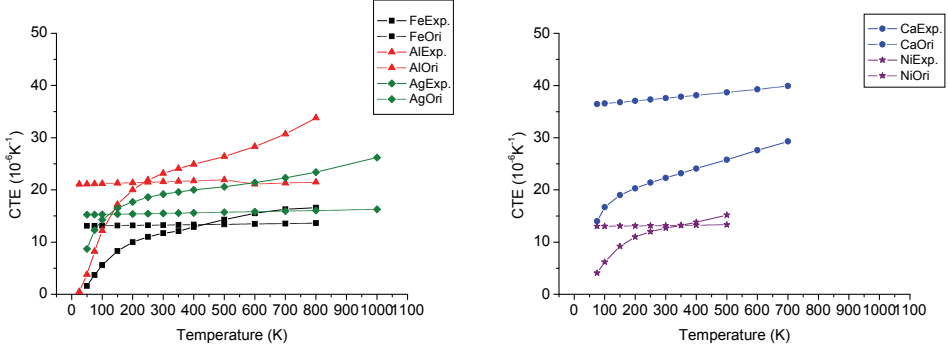


Figure 3: Comparison of temperature-dependent CTE between original Morse potential and experiments

modified Morse potential is developed as following:

$$E(r_{ij}) = D \left[ e^{-2\alpha(r_{ij}-r_0)} - A(T) e^{-\alpha(r_{ij}-r_0)} \right] \quad (6)$$

In Eq. (6), the constant of the attractive term is replaced by a temperature-related function  $A(T)$ . After substituting the modified Morse potential into the energy

equation  $\Delta E = 1/2k_B T$ , the solved vibration amplitudes are described as following:

$$r_1 = \frac{\alpha r_0 - \ln \left( \frac{1}{4D} * \left( 2DA(T) + 2\sqrt{\left( D^2A(T)^2 + 2Dk_B T - 4D^2A(T) + 4D^2 \right)} \right) \right)}{\alpha}$$

$$r_2 = \frac{\alpha r_0 - \ln \left( \frac{1}{4D} * \left( 2DA(T) - 2\sqrt{\left( D^2A(T)^2 + 2Dk_B T - 4D^2A(T) + 4D^2 \right)} \right) \right)}{\alpha} \quad (7)$$

In this study, the second-order polynomial equation is applied to determine the undefined function  $A(T)$ .

$$E(r_{ij}) = D \left[ e^{-2\alpha(r_{ij}-r_0)} - (a_0 + a_1 T + a_2 T^2) e^{-\alpha(r_{ij}-r_0)} \right] \quad (8)$$

where  $a_0$ ,  $a_1$ , and  $a_2$  are curve-fitted by the experimental data [Davis (1990); Gray (1973); Lide (2002)], and Table II shows the parameters of the modified Morse potential function.

Table 2: The parameters of modified Morse potential

Element	$a_0$	$a_1$	$a_2$
Na	2.01921	$16.696 * 10^{-5}$	$10.968 * 10^{-8}$
Cr	2.00379	$3.7781 * 10^{-5}$	$-4.7839 * 10^{-8}$
Fe	2.00432	$0.63508 * 10^{-5}$	$-4.5863 * 10^{-8}$
Mo	2.001177	$2.2493 * 10^{-5}$	$-2.2123 * 10^{-8}$
Ba	2.002339	$25.681 * 10^{-5}$	$-24.736 * 10^{-8}$
W	2.00083	$1.3114 * 10^{-5}$	$-1.0097 * 10^{-8}$
Al	2.00379	$0.64463 * 10^{-5}$	$-10.8 * 10^{-8}$
Ca	2.007344	$11.901 * 10^{-5}$	$-8.3558 * 10^{-8}$
Ni	2.005466	$0.10218 * 10^{-5}$	$-5.0596 * 10^{-8}$
Cu	2.000231	$1.0371 * 10^{-5}$	$-4.7982 * 10^{-8}$
Ag	2.003773	$-1.7284 * 10^{-5}$	$-5.3719 * 10^{-8}$
Pb	2.002602	$-4.673 * 10^{-5}$	$-7.2574 * 10^{-8}$

In the case of the fitting result of aluminum element, the value of  $A(T)$  slightly varies from 2.006 to 1.94 when different temperatures are applied. Figure (4) depicts the calculated CTE of Fe, Al, Ag, Ca, and Ni metals with modified Morse potential. Thus, comparing the original Morse potential with the modified Morse potential, it is observed that the modified Morse potential addresses the temperature-dependent thermal expansion problem of metals.

For an anharmonic oscillator shown in Fig. 1, it is difficult to calculate the average position. In this study, the assumption of  $(r_2 - r_1)/2$  being the average position, which is not far away from the exact average position of a Morse oscillator, is applied to simplified the complexity of the problem. One can get a more accurate solution through this procedure once the true average position is obtained.

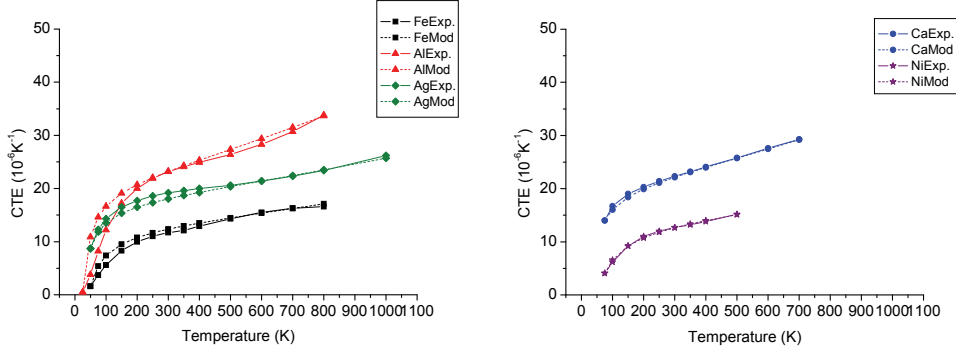


Figure 4: Comparison of temperature-dependent CTE between modified Morse potential and experiments

### 3 Temperature-Dependent Elastic Constant Calculation

Based on the SSSL model [Chiang, Chou, Wu and Yuan (2006)], an extensive study is proposed herein to investigate the temperature-dependent elastic constant of metals. This model assumes that the average position of atomic vibration of solid elements can be treated as the positions that achieve minimum total energy. All interatomic forces, which are described by Morse potential function, can be transferred into atomic springs from metallic lattice structure. Through the transformation, the originally discrete atomic structure can therefore be analyzed in the continuum level. Moreover, with the assumption of symmetric boundary conditions, the SSSL model can be considered as an infinitely repeated cubic structure, which assumes that the mechanical behavior is close to the bulk material.

Morse potential, as shown in Eq. (1), is adopted to describe the relationship of potential energy versus the distance of the diatom system, as well as to depict the relationship of bond strength versus diatoms distance. The force constants or bond strengths  $k(r_{ij})$  of the atomic springs are the second derivative of potential energy  $E(r_{ij})$ , as shown in Eq. (9)

$$k(r_{ij}) = \frac{d^2 E(r_{ij})}{dr_{ij}^2} = 2\alpha^2 D \left[ 2e^{-2\alpha(r_{ij}-r_0)} - e^{-\alpha(r_{ij}-r_0)} \right] \quad (9)$$

Figure (5) shows the atomic spring network of BCC and FCC lattice. In the BCC structure, there are one body-centered atom and eight corner atoms in a single cubic lattice. With the assumption of symmetric boundary conditions, six virtual nodes are illustrated in the center of the edge surfaces to evaluate the interatomic forces between adjacent body-centered atoms. The SSSL model is therefore illustrated including one body-centered node  $B$ , eight corner nodes,  $C_1$  to  $C_8$ , six virtual nodes,  $V_1$  to  $V_6$ , and three sets of atomic springs, as shown in Fig. 5(a). The spring set 1,  $\overline{BC_1}$  to  $\overline{BC_8}$ , is the center-corner spring which represents the interatomic forces between the body-centered atom and the eight corner atoms with initial lengths of  $r_0$ . The spring set 2,  $\overline{C_1C_2}$  to  $\overline{C_7C_8}$ , is the corner-corner spring which represents the interatomic forces between adjacent corner atoms with initial lengths of  $2r_0 \cos \theta$  where  $\theta$  represents the angle between the center-corner spring and corner-corner spring. The spring set 3,  $\overline{BR_1}$  to  $\overline{BR_6}$ , is the center-center spring which represents the interatomic forces between adjacent body-centered atoms with initial lengths of  $r_0$ .

Similarly, in FCC structure, the SSSL model is illustrated including the face-centered nodes  $F_1$  to  $F_6$  and the corner nodes  $C_1$  to  $C_8$  as shown in Fig. 5(c). The interatomic forces in the FCC structure are transferred into four sets of atomic springs. The spring set 1,  $\overline{F_1C_1}$  to  $\overline{F_6C_8}$ , is the center-corner spring which represents the interatomic forces between the adjacent face-centered atoms and corner atoms with initial lengths of  $r_0$ . The spring set 2,  $\overline{F_1F_2}$  to  $\overline{F_5F_6}$ , is the A-center spring which represents the interatomic forces between the adjacent face-centered atoms with initial lengths of  $r_0$ . The spring set 3,  $\overline{C_1C_2}$  to  $\overline{C_7C_8}$ , is the corner-corner spring which represents the interatomic forces between the adjacent corner atoms with initial lengths of  $2r_0 \cos \theta$  where  $\theta$  represents the angle between the center-corner spring and corner-corner spring. The spring set 4,  $\overline{F_1F_6}$ ,  $\overline{F_2F_4}$ ,  $\overline{F_3F_5}$ , is the C-center spring which represents the interatomic forces between the across face-centered atoms with initial lengths of  $2r_0 \cos \theta$ .

By applying a small prescribed extension on the top nodes of SSSL model, the elastic constants of cubic metals are calculated in the following equations.

$$E_{BCC} = \frac{2\alpha^2 D \left[ 8 + 15 \left( 2e^{-2\left(\frac{2}{\sqrt{3}}-1\right)\alpha r_0} - e^{-\left(\frac{2}{\sqrt{3}}-1\right)\alpha r_0} \right) \right]}{\sqrt{3}r_0} \quad (10)$$

$$E_{FCC} = \frac{10\alpha^2 D \left[ 1 + \left( 2e^{-2(\sqrt{2}-1)\alpha r_0} - e^{-(\sqrt{2}-1)\alpha r_0} \right) \right]}{\sqrt{2}r_0}$$

Equation (10) shows that the elastic constant could be simply estimated by three Morse potential parameters, namely,  $\alpha$ ,  $D$ , and  $r_0$ . The calculated elastic constant



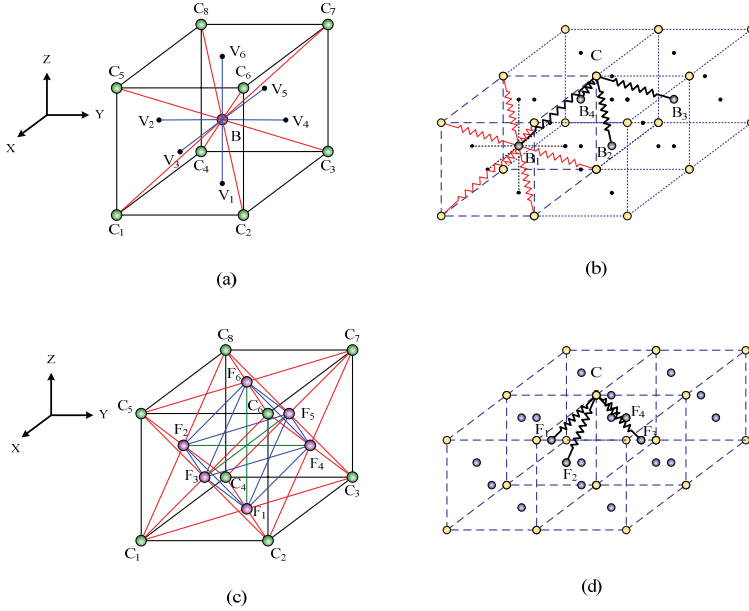


Figure 5: Simple-spring-single-lattice model construction. (a) The SSSL model for the BCC structure (b) Sketch of reaction force calculation for the BCC structure (c) The SSSL model for the FCC structure (d) Sketch of reaction force calculation for the FCC structure

of SSSL models are shown in Fig. 6 where the Morse potential parameters  $\alpha$ ,  $D$ , and  $r_0$  in Table 1 are adopted. To compare with the bulk values [Gschneider (1964); Kaye and Laby (1995); Lide (2002)], the elastic constants of most metals obtained by SSSL model are close to the bulk value.

In Morse potential, the parameter  $r_0$  indicates the diatom distance at the lowest energy state, as well as the distance of vibration center of diatoms. When the temperature increases, the anharmonic oscillators between atoms start to vibrate. The distance of vibration centers  $\bar{r}_0$  becomes larger which means the bond strength  $k(r_{ij})$  varies with temperature. Equation (4) shows vibration amplitudes  $r_1$  and  $r_2$  of Morse oscillator at temperature  $T$ , and we assume the diatom distance of vibration centers is  $\bar{r}_0 = (r_1 + r_2)/2$ . After substituting  $\bar{r}_0$  into Eq. (10) to replace the parameter  $r_0$ , temperature-dependent elastic constants of cubic metals are evaluated. In this study, both original Morse function and aforementioned modified Morse function are taken into account in temperature-dependent elastic constant calculation. In the elastic constant calculation, all Morse parameter sets shown in Table

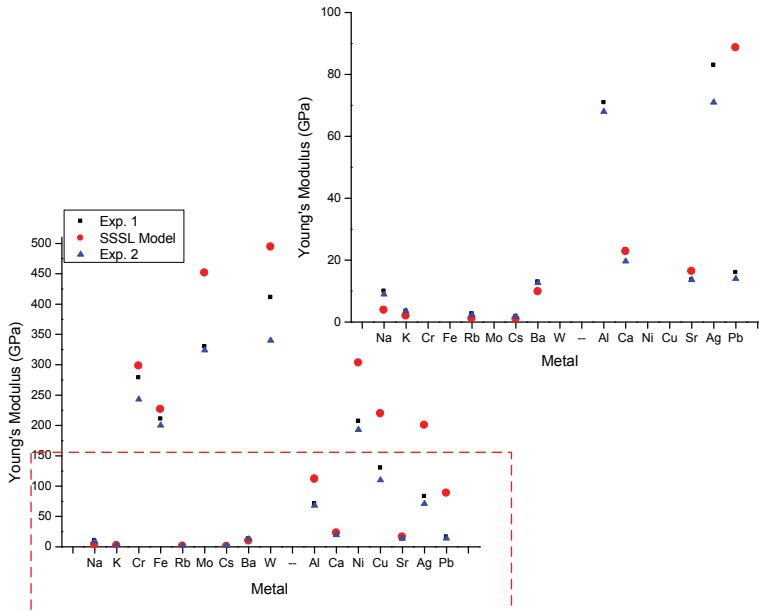


Figure 6: The calculation results of the SSSL model for Girifalco's potential parameter set

I were analyzed. Taking Cu (FCC structure) and Fe (BCC structure) as examples, the calculation results as against the experimental data [Ledbetter (1977); Rayne and Chandrasekhar (1961)] are shown in Figure (7) and (8). The results show that an agreement is achieved on trends between the predicted elastic constants and the corresponding experimental data. Moreover, the results of the modified Morse potential do not show obvious difference from the original Morse potential.

The reason deduced is that the modified Morse potential is applied to adjust the material properties of CTE, which is much sensitive to temperature than elastic constant. In CTE model, The CTE is determined by the average position of Morse oscillator as shown in Eq. 5. In SSSL model, the elastic constant calculation is the combination of the second differentiation of Morse potential, as shown in Eq. 10. The average position of Morse oscillator varies dramatically when the potential energy from zero to the dissociation energy  $D$ . However, the variation of the second differentiation of Morse potential is not as much as the average position.

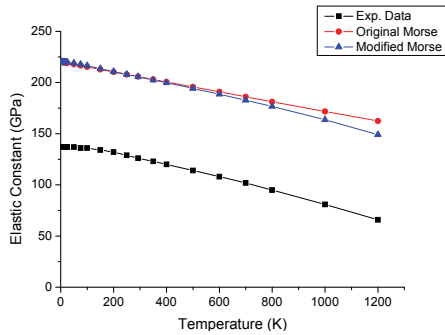


Figure 7: The calculation results of temperature-dependent elastic constant of Cu metal

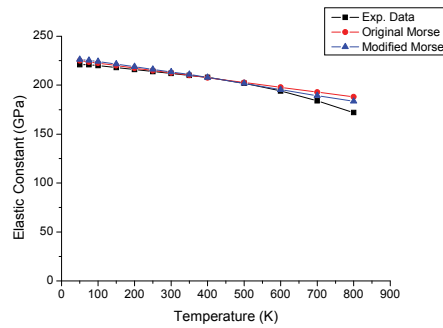


Figure 8: The calculation results of temperature-dependent elastic constant of Fe metal

#### 4 Conclusion

In this study, two temperature-dependent material properties of cubic metals, the thermal expansion coefficient and the elastic constant, were analyzed using anharmonic oscillator networks; several closed-form analytical equations were developed. The interatomic forces are treated as anharmonic oscillators; the originally discrete atomic structure can therefore be analyzed in the continuum level.

In the investigation of thermal expansion coefficient, the result showed that the closed-form solution using the original Morse potential can give a good prediction of the CTE of metals at room temperature; however, it is not adequate to use its temperature-insensitive parameters to predict the CTE at low temperature and at high temperature; a modified Morse potential is therefore proposed and developed to describe the nature of the thermomechanical behavior of metals. The calculated CTE using modified Morse potential can meet the experimental data quantitatively.

In the investigation of elastic constant, an agreement on trends between the predicted elastic constants and the corresponding experimental data is also achieved. Besides, different from CTE calculation results, the results of elastic constant calculation show that there is no significant discrepancy between original Morse potential and modified Morse potential application. Though the SSSL-based model much reduces the complexity of the real bulk metals including their defects, dislocations, etc., it provides a feasible way to estimate temperature-dependent properties within a reasonable range.

In the case of SSSL computation, after the closed-form solution is established, both original Morse potential and modified Morse potential can be taken into consideration immediately. Through the analyzing procedure, one can make a prompt

estimate on the material properties such as the CTE and elastic constant, once the potential function and lattice structure are determined.

## References

**Chiang, K. N.; Chou, C. Y.; Wu, C. J.; Yuan, C. A.** (2006): Prediction of the bulk elastic constant of metals using atomic-level single-lattice analytical method, *Appl. Phys. Lett.*, vol. 88, 171904.

**Davis, J. R.** (1990): *Metals Handbook*, 10<sup>th</sup> ed.

**Daw, M. S.; Baskes, M. I.** (1984): Embedded-atom method: Derivation and application to impurities, surfaces, and other defects in metals, *Phys. Rev. B*, vol. 29, 6443.

**Foiles, S. M.; Daw, M. S.** (1988): Calculation of the thermal expansion of metals using the embedded atom method, *Phys. Rev. B*, vol. 38, 12643.

**Girifalco, L. A.; Weizer, V. G.** (1959): Application of the Morse potential function to cubic metals, *Phys. Rev.*, vol. 114, pp. 687-690.

**Gray, D. E.** (1973): *American Institute of Physics Handbook*, 2<sup>nd</sup> ed.

**Gschneider Jr., K. A.** (1964): Physical Properties and Interrelationships of Metallic and Semimetallic Elements, *Solid State Phys.*, vol. 16, 276.

**Jeng, Y. R.; Tan, C. M.** (2002): Theoretical study of dislocation emission around a nanoindentation using a static atomistic model, *Phys. Rev. B*, vol. 65, 174101.

**Kaye, G. W. C.; Laby, T. H.** (1995): *Tables of Physical and Chemical Constants*.

**Ledbetter, H. M.** (1977): Elastic Properties of Zinc: A Compilation and a Review, *J. Phys. Chem. Ref. Data*, vol. 6, pp. 1181-1203.

**Lide, D. R.** (2002): *CRC Handbook of Chemistry and Physics*, 83<sup>rd</sup> ed.

**Park J. Y.; Cho Y. S.; Kim S. Y. ; Jun S.; Im S.** (2006): A Quasicontinuum Method for Deformations of Carbon Nanotubes, *CMES: Computer Modeling & Engineering Science*, Vol. 11, No. 2, pp. 61-72.

**Rayne, J. A.; Chandrasekhar, B. S.** (1961): Elastic Constants of Iron from 4.2 to 300°K, *Phys. Rev.*, vol. 122, 1714.

**Theodosiou T. C.; Saravanos D. A.** (2007): Molecular Mechanics Based Finite Element For Carbon Nanotube Modeling, *CMES: Computer Modeling & Engineering Science*, Vol. 19, No. 2, pp. 121-134.